the plant journal

SEB Society for Experimental Biology

The Plant Journal (2017) **90,** 573–586 doi: 10.1111/tpj.13514

Transcriptome analysis of the *Brassica napus–Leptosphaeria maculans* pathosystem identifies receptor, signaling and structural genes underlying plant resistance

Michael G. Becker[1,†], Xuehua Zhang[2,†], Philip L. Walker[1], Joey C. Wan[1], Jenna L. Millar[1], Deirdre Khan[1], Matthew J. Granger[1], Jacob D. Cavers[1], Ainsley C. Chan[1], Dilantha W.G. Fernando[2] and Mark F. Belmonte[1,*]

[1]*Department of Biological Sciences, University of Manitoba, Winnipeg, MB R3T2N2, Canada, and*

[2]*Department of Plant Science, University of Manitoba, Winnipeg, MB R3T2N2, Canada*

Received 16 May 2016; revised 5 February 2017; accepted 10 February 2017; published online 21 February 2017.

*For correspondence (e-mail mark.belmonte@umanitoba.ca).

†These authors contributed equally to this work.

SUMMARY

The hemibiotrophic fungal pathogen *Leptosphaeria maculans* is the causal agent of blackleg disease in *Brassica napus* (canola, oilseed rape) and causes significant loss of yield worldwide. While genetic resistance has been used to mitigate the disease by means of traditional breeding strategies, there is little knowledge about the genes that contribute to blackleg resistance. RNA sequencing and a streamlined bioinformatics pipeline identified unique genes and plant defense pathways specific to plant resistance in the *B. napus–L. maculans LepR1–AvrLepR1* interaction over time. We complemented our temporal analyses by monitoring gene activity directly at the infection site using laser microdissection coupled to quantitative PCR. Finally, we characterized genes involved in plant resistance to blackleg in the Arabidopsis–*L. maculans* model pathosystem. Data reveal an accelerated activation of the plant transcriptome in resistant host cotyledons associated with transcripts coding for extracellular receptors and phytohormone signaling molecules. Functional characterization provides direct support for transcriptome data and positively identifies resistance regulators in the Brassicaceae. Spatial gradients of gene activity were identified in response to *L. maculans* proximal to the site of infection. This dataset provides unprecedented spatial and temporal resolution of the genes required for blackleg resistance and serves as a valuable resource for those interested in host–pathogen interactions.

Keywords: blackleg, resistance, transcriptome, RNA sequencing, *Brassica napus*, *Leptosphaeria maculans*, laser microdissection.

INTRODUCTION

Brassica napus (canola, oilseed rape) is the second most widely produced oilseed crop worldwide and is under constant threat of blackleg disease caused by the hemibiotrophic fungal pathogen *Leptosphaeria maculans* (Fitt *et al.*, 2006). Currently, mitigation of crop loss relies largely on race-specific resistance (*R*) genes and their corresponding pathogen avirulence (*Avr*) genes (Larkan *et al.*, 2015). Interaction between the products of *R* and *Avr* results in an incompatible host–pathogen interaction and pathogen restriction from host tissues. Absence of either the *R*- or the *Avr* gene results in a compatible host–pathogen interaction and colonization of the host. Each interaction is probably governed by large sets of genes activated over time and under the control of cellular receptors and signal transduction cascades that determine host fate. Although *R*-genes conferring blackleg resistance have been identified in canola (Marcroft *et al.*, 2012; Larkan *et al.*, 2013), it is unclear by which mechanisms these genes effectively inhibit *L. maculans* colonization. Previous transcriptome studies of the *B. napus–L. maculans* pathosystem limit analyses to compatible interactions and focus on pathogen virulence and effectors (Lowe *et al.*, 2014; Haddadi *et al.*, 2016). Thus, there is a critical need to identify the genes facilitating host resistance against *L. maculans* and define how the host defense response is controlled in both space and time.

Plant defense response mechanisms are commonly subdivided into two immune pathways: pattern-triggered immunity (PTI) and effector-triggered immunity (ETI) (Jones and Dangl, 2006; Thomma *et al.*, 2011). PTI is characterized by the

detection of pathogen-associated molecular patterns (PAMPs) via extracellular membrane receptors such as receptor-like proteins (RLPs) and receptor-like kinases (RLKs), while ETI is characterized by the detection of pathogen effectors or their perturbation of host molecules by intracellular nucleotide-binding–leucine-rich repeat (NB-LRR) receptors (Tsuda and Katagiri, 2010; Dangl *et al.*, 2013). Both immune pathways share cellular machinery to elicit a defense response; however, PTI is associated with non-host resistance and ETI (in conjunction with PTI) with host incompatibility (Bigeard *et al.*, 2015). Although it is a useful model, this ETI/PTI dichotomy cannot be effectively applied to the Arabidopsis- or *B. napus*–*L. maculans* pathosystems. Not only are effector-triggered NB-LRR receptors required for Arabidopsis non-host resistance to *L. maculans* (Staal *et al.*, 2006), but the recently cloned *B. napus R*-gene, *LepR3*, has been identified as a transmembrane RLP (Larkan *et al.*, 2013). Thus, effector-triggered defense (ETD) was proposed by Stotz *et al.* (2014) and refers specifically to RLP-triggered incompatible interactions. Unlike the rapid cell death observed in ETI, ETD is often associated with a delayed onset of cell death, as observed in *B. napus*–*L. maculans* incompatible interactions (Stotz *et al.*, 2014). As *L. maculans* grows apoplastically, the ability of *R*-gene products to detect pathogens in the extracellular space is logical and supports the ETD paradigm.

Following the recognition of hemibiotrophic pathogens, early defense responses such as the activation of mitogen-activated protein kinases (MAPKs) are triggered within the cell (Meng and Zhang, 2013). Subsequently, large-scale transcriptional reprogramming contributes to the regulation of phytohormone signaling pathways (Denancé *et al.*, 2013). Jasmonic acid (JA) and abscisic acid (ABA) are both involved in Arabidopsis non-host resistance to *L. maculans* (Kaliff *et al.*, 2007), and JA, ethylene (ET) and salicylic acid (SA) signaling pathways are activated during the *B. napus*–*L. maculans* host–incompatible interaction (Šašek *et al.*, 2012). Although hormone signaling has been described temporally across the plant defense response to fungal pathogens (reviewed in Mishra *et al.*, 2012), there are no data on the spatial partitioning of these genes following ETD in host tissues.

Downstream plant defense responses in hemibiotrophic pathosystems may involve the deposition of callose (Ellinger *et al.*, 2013). Callose deposition is typically triggered by PAMPs, and PAMP-induced callose deposition has been used as a marker for PTI activity in Arabidopsis (Luna *et al.*, 2011). Indole glucosinolates (IGS), bioactive secondary metabolites with anti-fungal capabilities, also promote the production of callose (Clay *et al.*, 2009). In Arabidopsis, resistance to hemibiotrophic fungi can be dependent on the production of IGS (Hiruma *et al.*, 2013) or callose deposition (Staal *et al.*, 2006; Kaliff *et al.*, 2007); however, their role in the *B. napus*–*L. maculans* pathosystem remains unclear.

We profiled the transcriptome of *B. napus* cotyledons inoculated with *L. maculans* across a 2-week infection period to explore the activation of ETD pathways and identify specific regulators and genes contributing to host resistance. Detailed anatomical observations complement our molecular analyses and clearly show the delayed onset of cell death indicative of ETD. Genes activated exclusively in resistant cotyledons were disrupted in Arabidopsis and positively identify uncharacterized receptors, negative cell death regulators and activators of sulfur metabolism that contribute to *L. maculans* defense in the Brassicaceae. We explored the activity of these genes and defense markers directly at, and proximal to, the infection site. Data show tightly controlled spatial transcriptional gradients developed during ETD that are associated with pathogen detection, IGS production and hormone signaling. Taken together, our data provide a global transcriptome analysis of ETD against *L. maculans* and show early activation of defense pathways in resistant cotyledons that are controlled in space and time.

RESULTS

The *LepR1*–*AvrLepR1* gene interaction is responsible for resistance in DF78 cotyledons

To better understand the host–pathogen relationship between *B. napus* and *L. maculans*, we performed cotyledon inoculation assays based on the gene-for-gene model developed by Flor (1971) and frequently applied in the characterization of *R*-genes (Rouxel *et al.*, 2003; Marcroft *et al.*, 2012). A total of 34 characterized *L. maculans* isolates were tested against 104 *B. napus* varieties/lines (Zhang *et al.*, 2016). We selected resistant line DF78 (LepR1) for further analysis because of its strong defense response against *L. maculans* (AvrLepR1) and our interest in the poorly characterized *R*-gene *LepR1*. Our results show that DF78 is resistant to all isolates carrying *AvrLepR1* or *AvrLm3*. As the *L. maculans* isolate D3 used for this study does not carry *AvrLm3* (Table S1 in the Supporting Information; Zhang *et al.*, 2016), the response of DF78 cotyledons to the D3 *L. maculans* isolate must be the result of a *LepR1*–*AvrLepR1* gene interaction. To confirm this, *B. napus* variety Q2 (*Rlm3*; Van de Wouw *et al.*, 2010) and *B. napus* line 1065 (*LepR1*; Zhang *et al.*, 2016) were used as controls. When the Westar cultivar was challenged with all 34 isolates, no resistance was observed, confirming previous reports that Westar is universally susceptible to *L. maculans* (Table S1).

Phenotypic and cellular characterization of *B. napus* cotyledons in response to *L. maculans* infection

Next we examined the phenotypic characteristics of resistant (DF78; LepR1) and susceptible (Westar) *B. napus* hosts infected with *L. maculans* (Figure 1a). Lesions spread rapidly in susceptible cotyledons at 7 days post-inoculation

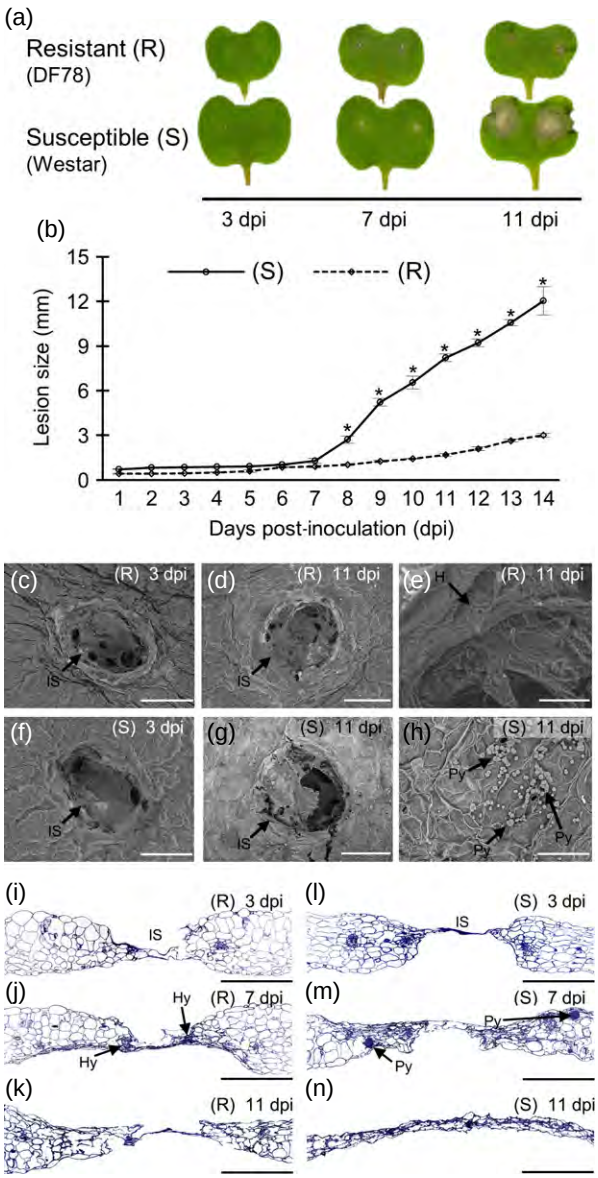

Figure 1. Disease symptoms in *Brassica napus* cotyledons in response to *Leptosphaeria maculans* infection.
(a) Disease symptoms in resistant (R) and susceptible (S) cotyledons at 3, 7 and 11 days post inoculation (dpi). (b) Lesion size over time. Asterisks ($P < 0.01$, Student's *t*-test). Scanning electron micrograph (SEM) of R at 3 dpi (c) and 11 dpi (d) at the infection site (black arrow): scale = 1 mm. (e) Fungal hyphae (H) at infection site: scale = 50 μm in R at 11 dpi. (f, g) SEM of S at 3 dpi (f) and 11 dpi (g) at the infection site (IS): scale = 1 mm. (h) SEM of pycnidia (Py) on S cotyledons at 11 dpi: scale = 200 μm. (i–n) Light micrographs of R at 3 dpi (i), 7 dpi (j), 11 dpi (k) and S at 3 dpi (l), 7 dpi (m) and 11 dpi (n): scale bars = 500 μm.

(dpi), while in resistant hosts lesion size only slightly increased towards the end of the 14-day infection period (Figure 1b). Scanning electron and light microscopy of resistant cotyledons showed minimal cellular breakdown adjacent to the infection site at 3 and 7 dpi (Figure 1c,d,i,j), as is characteristic of ETD responses, despite the presence of fungal hyphae within the infection site (Figure 1e), and by 11 dpi resistant hosts show marginal cellular degradation (Figure 1k). In susceptible hosts, cells adjacent to the infection site were intact at 3 dpi (Figure 1f) and widespread cell death by 7 (Figure 1m) and 11 dpi (Figure 1g,n) with fungal fruiting bodies being clearly visible (Figure 1h,m).

Global comparison of gene activity in the *B. napus*–*L. maculans* pathosystem

To identify genes responsible for resistance of *B. napus* to *L. maculans*, we profiled the transcriptomes of resistant and susceptible cotyledons using next-generation RNA sequencing across a 2-week infection period. First, hierarchical clustering analysis revealed relationships between genotypes and in response to *L. maculans* infection (Figure 2a). Treatments generally grouped according to genotype at 0–3 dpi, apart from infected resistant cotyledons at 3 dpi that cluster with susceptible plants at 7 dpi, suggesting an accelerated defense response. Towards the latter stages of the infection process, treatments form a clade based largely on exposure to *L. maculans*, highlighting global shifts in gene expression in both genotypes following pathogen attack. Mock-inoculated resistant plants at 11 dpi were also placed within this clade, which may be related to its developmental profile and shared activation of senescence-associated genes.

Figure 2(b) summarizes transcript populations in both genotypes and across treatments. Transcript abundance was measured as fragments per kilobase of gene per million mapped reads (FPKM) where a gene was scored as 'expressed' when FPKM ≥1 (Mortazavi *et al.*, 2008; Trapnell *et al.*, 2012; Bhardwaj *et al.*, 2015). Regardless of genotype or treatment, the number of active genes was similar, with an average of 41 110 expressed genes (41% of the *B. napus* gene models). Transcript abundance was scored as low (FPKM ≥1 to <5), moderate (FPKM ≥5 to <25) or high (FPKM ≥25), with the majority of transcripts detected at low (53%) or moderate (36%) levels. Cumulatively, 57 654 transcripts were detected across all 12 treatments with an FPKM ≥1. The full annotation and all gene expression levels can be found in Data S1.

Thousands of genes are activated in *B. napus* in response to *L. maculans*

To identify those genes that contribute to plant resistance, differential gene expression analysis was performed at all stages of the 11-day infection process in both resistant and susceptible hosts and data were compared with their respective mock, water-inoculated controls. At 3, 7 and 11 dpi, we detected a total of 1992, 3234 and 4173 upregulated differentially expressed genes (DEGs; $P < 0.05$) in resistant hosts and 571, 3873 and 8489 upregulated DEGs

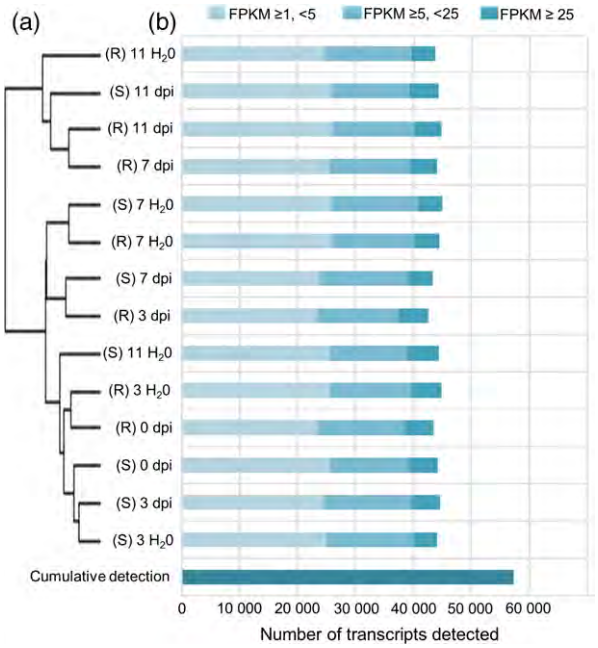

Figure 2. Hierarchical clustering and global gene activity in the *Brassica napus–Leptosphaeria maculans* pathosystem.
(a) Hierarchical clustering of all differentially expressed genes detected in the dataset.
(b) Number of transcripts detected in both genotypes across all treatments. Transcripts with an FPKM (fragments per kilobase of gene per million mapped reads) >1 are considered to be detected. Detected transcripts are subdivided into low (FPKM ≥1 to <5), moderate (FPKM ≥5 to <25) or high (FPKM ≥25) detection levels.

in susceptible hosts, respectively (Figure 3a–c). The number of DEGs shared between resistant and susceptible host cotyledons also increased over time, probably due to the total number of DEGs between treatments. A complete summary of all DEGs, both up- and downregulated, can be found in Data S2.

Host resistance is associated with pathogen recognition, cell signaling and vesicular trafficking in resistant plants

To identify the biological processes, molecular functions and cellular components contributing to host resistance against *L. maculans*, we performed Gene Ontology (GO) term enrichment on all upregulated DEG sets (Figure 3d, Data S3). The DEGs identified in resistant cotyledons at 3 dpi are enriched with kinase activity ($P = 1.05 \times 10^{-13}$), signal transduction ($P = 1.5 \times 10^{-4}$) and plasma membrane ($P = 2.85 \times 10^{-30}$), and code for wall-associated kinases (WAKs), RLKs, RLPs, LRR-NBS receptors, and transducers of signaling such as MAPKs and MAPK kinases (MKK). Specifically, we identified two putative homologs of *RLP30* (*BnaA06g12200D*, *BnaA06g12220D*), receptor complex regulator *SUPPRESSOR OF BIR1 1* (*SOBIR1*, *BnaA03g14760D*, *BnaCnng39490D*) and homologs of signal transducer *MKK9* (*BnaA02g35860D*, *BnaC02g22230D*) that were upregulated specifically in resistant cotyledons at 3 dpi (Table 1).

SA and JA signaling are strongly affected by the *LepR1–AvrLepR1* gene interaction

RNA sequencing and GO term enrichment identified DEGs in resistant cotyledons at 3 dpi associated with the SA-mediated signaling pathway ($P = 6.70 \times 10^{-18}$), ET-mediated signaling pathway ($P = 6.57 \times 10^{-12}$), and JA-mediated signaling pathway ($P = 2.48 \times 10^{-65}$; Figure 3d). To further characterize the temporal regulation of hormone production and signaling in response to *L. maculans*, we examined transcript levels of hormone biosynthetic genes and markers for SA, ET, JA, ABA and auxin across the infection process in both genotypes (Figure S1).

Expression of SA biosynthetic gene *ISOCHORISMATE SYNTHASE 1* homologs, in addition to SA marker *PATHOGENESIS-RELATED GENE 1* (PR1), increased an average of 5.01-fold against the mock at 3 dpi in resistant plants, compared with an increase of 1.26-fold in their susceptible counterparts. Data show an increased abundance of transcripts related to ET/JA biosynthesis and signaling by 3 dpi in resistant cotyledons, including *ACC OXIDASE 2* (*BnaA09g13300D*, *BnaC09g13570D*) and the ET-JA marker *PDF1.2* (*BnaA07g32130D*, *BnaC02g23620D*), that continued to accumulate across the infection process. Remarkably, in susceptible hosts, expression levels of several JA-biosynthetic genes decreased. For example, the expression of *LIPOXEGENASE 2* (*LOX2*; *BnaA07g24870D*, *BnaA07g24880D*), *ALLENE OXIDE SYNTHASE* (*AOS*; *BnaC02g29610D*) and *ALLENE OXIDE CYCLASE 3* (*AOC3*; *BnaC09g52550D*) decreased an average of 4.01-fold compared with mock controls at 7 and 11 dpi (Figure S1). Finally, expression of auxin (*NITRILASE 2*, *BnaA06g38980D*, *BnaC02g07040D*, *BnaC03g54910D*, *BnaCnng75490D*) and ABA (*NINE-CIS-EPOXYCAROTENOID DIOXYGENASE 3*, *BnaA01g29390D*, *BnaC01g36910D*, *BnaC05g39200D*) markers increased in susceptible cotyledons at 11 dpi, and may be the result of widespread cell death late in the infection process (Figure 1n).

Regulation of cell death is associated with ETD against *L. maculans*

We identified DEGs associated with negative regulation of programmed cell death ($P = 4.76 \times 10^{-76}$) upregulated specifically in resistant hosts at 3 dpi (Table 1), including putative homologs of *BAX INHIBITOR 1* (*BnaC09g20030D*), *BOTRYTIS SUSCEPTIBLE 1 INTERACTOR* (*BnaC01g41070D*), *DEVELOPMENT AND CELL DEATH 1* (*BnaA07g15670D*), *NUDIX HYDROXYLASE HOMOLOG 7* (*BnaC03g22580D*), *METACASPASE 2* (*BnaA01g14460D*) and *NECROTIC SPOTTED LESIONS 1* (*BnaC03g58590D*). Activation of cell death regulators early during ETD may limit lesion spread following the biotrophic–necrotrophic transition of *L. maculans*.

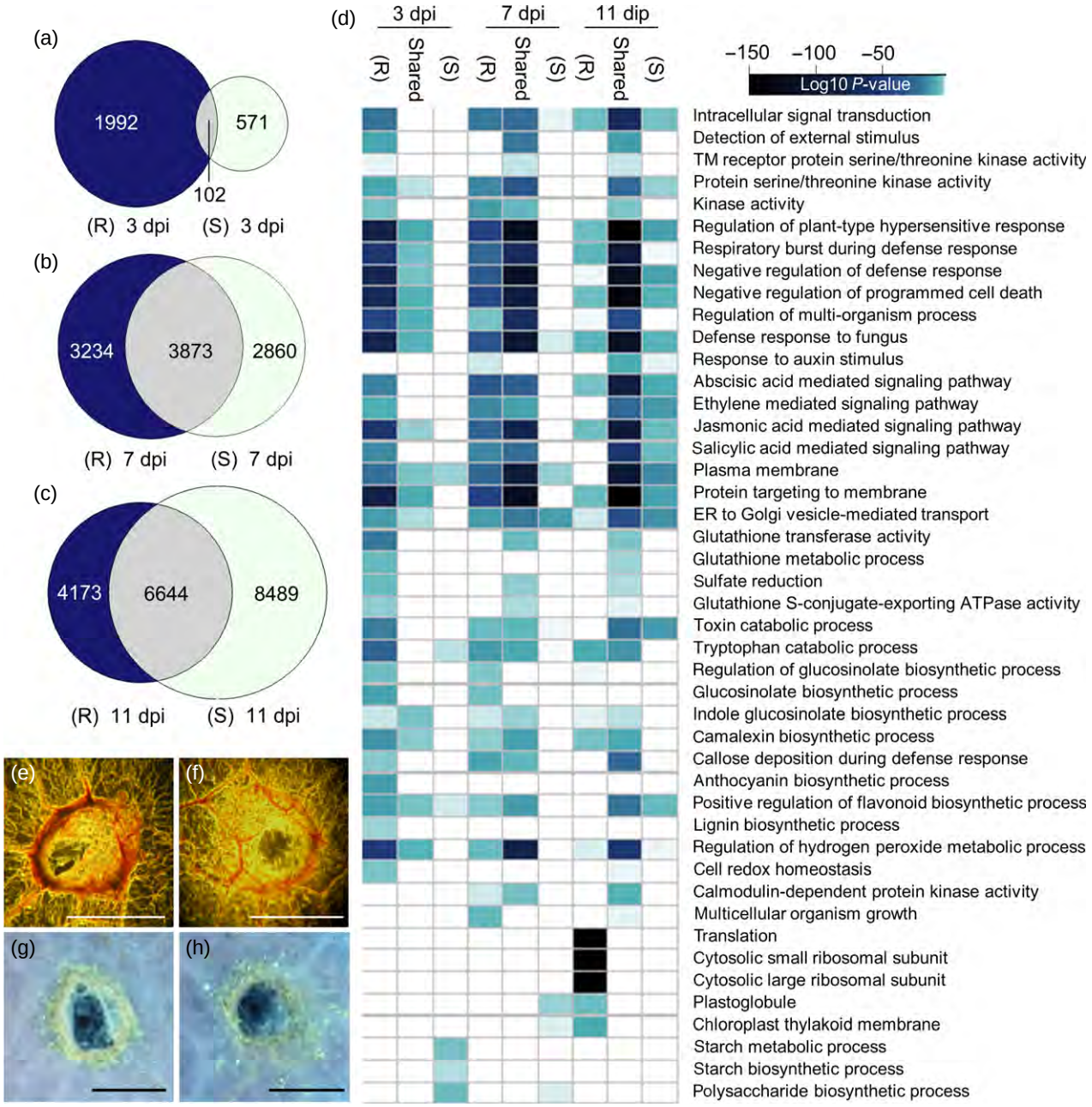

Figure 3. Upregulated differentially expressed genes in resistant (R) and susceptible (S) *Brassica napus* cotyledons inoculated with *Leptosphaeria maculans* as compared with mock inoculated controls.
(a–c) Venn diagram showing activated genes at (a) 3, (b) 7 and (c) 11 days post-inoculation (dpi) in response to *L. maculans* in R (left), S (right) or shared between both genotypes (intersect). (d) Heatmap of enriched Gene Ontology terms identified from upregulated genes. Terms are considered enriched at $P < 0.001$. A darker blue color represents a greater statistical enrichment. (e, f) Deposition of lignified plant materials at the site of infection in R (e) and S (f) hosts at 7 dpi. Lignified plant materials appear dark orange/red. (g, h) Aniline blue callose staining of R (g) and S (h) *B. napus* cotyledons inoculated with *L. maculans* at 7 dpi. Scale bars = 1 mm.

Rapid activation of genes associated with sulfur metabolism

DEGs associated with sulfate reduction ($P = 1.51 \times 10^{-7}$), sulfate assimilation ($P = 1.14 \times 10^{-11}$) and glutathione metabolic process ($P = 8.64 \times 10^{-8}$) were identified specifically in resistant cotyledons at 3 dpi (Figure 3d), including sulfur assimilators *APS REDUCTASE* (*APR1*, *BnaA09g20370D*, *BnaC09g22760D*), *APR2* (*BnaC04g 19270D*), *APR3* (*BnaC01g13420D*, *BnaC07g37060D*) and *SULFITE REDUCTASE* (*BnaC09g50680D*), as well as sulfate activators *ADENOSINE 5′-PHOSPHOSULFATE KINASE 1*

Table 1 Accumulation of transcripts during *Leptosphaeria maculans* infection in resistant (R) and susceptible (S) *Brassica napus* cotyledons. Significant ($P < 0.05$) decreases or increases in transcript abundance compared with mock controls are in bold

		Fold change versus mock control					
Brassica napus locus	Putative annotation	R 3 dpi	R 7 dpi	R 11 dpi	S 3 dpi	S 7 dpi	S 11 dpi
BnaA03g46200D	*PUTATIVE NBS-LRR RECEPTOR*	**2.16**	**6.03**	**3.02**	0.85	**10.46**	**26.07**
BnaC04g12970D	*PUTATIVE NBS-LRR RECEPTOR*	**2.12**	**3.55**	1.40	0.54	**2.40**	**12.61**
BnaA03g14760D	*SUPRESSOR OF BIR1 1*	**2.10**	**5.12**	**2.13**	1.43	**2.80**	**21.13**
BnaCnng39490D	*SUPRESSOR OF BIR1 1*	**2.99**	**3.86**	**3.19**	1.36	**3.74**	**7.21**
BnaC04g43230D	*RECEPTOR-LIKE PROTEIN 30*	**4.60**	**12.75**	**3.12**	0.70	**4.92**	**37.27**
BnaA06g12200D	*RECEPTOR-LIKE PROTEIN 30*	**2.97**	**5.90**	1.28	1.41	1.54	**12.65**
BnaA04g06980D	*CRK10*	**5.12**	**3.29**	**14.21**	0.42	0.82	**17.56**
BnaA02g21140D	*CRK39*	**5.20**	**41.07**	**10.07**	1.12	**27.26**	**205.9**
BnaA02g35860D	*MAP KINASE KINASE 9*	**2.00**	**2.86**	**2.30**	0.64	**1.72**	**12.94**
BnaC02g22230D	*MAP KINASE KINASE 9*	**5.39**	**5.27**	**2.41**	**0.40**	**4.90**	**25.43**
BnaA08g17130D	*SEC23/24 TRANSPORT GENE*	0.99	**2.40**	0.80	1.41	0.82	**2.20**
BnaC03g73490D	*SYNTAXIN OF PLANTS 121*	1.03	**1.71**	**1.86**	1.85	1.05	**7.90**
BnaA07g30760D	*KUNITZ TRYPSIN INHIBITOR 1*	**2.69**	**3.51**	**9.31**	0.59	**0.03**	**0.14**
BnaC09g20030D	*BAX INHIBITOR 1*	**1.82**	**3.08**	**4.53**	1.39	**11.54**	**38.20**
BnaC03g58590D	*NECROTIC SPOTTED LESIONS 1*	**1.70**	**1.98**	**1.70**	1.31	1.70	**19.29**
BnaC03g22580D	*NUDIX HYDROXYLASE H7*	**5.53**	**17.96**	**11.44**	1.54	**39.82**	**27.34**
BnaC01g41070D	*BOTRYTIS SUSCEPTIBLE 1 INTERACTOR*	**1.66**	1.08	1.18	0.64	0.69	**6.87**
BnaC06g13910D	*DEFENDER AGAINST DEATH 1*	**1.81**	**1.83**	**1.74**	1.28	0.55	**45.89**
BnaA07g15670D	*DEVELOPMENT AND CELL DEATH 1*	**2.73**	1.30	**2.20**	0.99	1.00	**28.99**
BnaC09g50680D	*SULFITE REDUCTASE 1*	**1.77**	**2.62**	0.97	0.69	1.29	**1.05**
BnaA03g38670D	*APK1*	**2.65**	**5.89**	**6.69**	1.27	0.81	**3.16**
BnaA01g34620D	*APK1*	**3.37**	**4.87**	**25.01**	0.59	0.83	2.15
BnaA09g20370D	*APS REDUCTASE 1*	**2.85**	**2.40**	**1.79**	1.14	**5.60**	**6.53**
BnaC09g22760D	*APS REDUCTASE 1*	**2.27**	1.19	1.32	1.24	**12.51**	**5.02**
BnaA06g28850D	*GLUTATHIONE SYNTHETASE 2*	**1.55**	**2.01**	**1.94**	0.99	1.64	**1.87**
BnaC07g27830D	*GLUTATHIONE SYNTHETASE 2*	**1.87**	**1.81**	**1.85**	1.03	0.84	**1.78**
BnaC09g40740D	*GLUTATHIONE S-TRANSFERASE PHI 12*	**10.46**	0.44	**0.25**	**0.20**	**10.13**	**0.09**
BnaA07g24870D	*LIPOXYGENASE 2*	1.00	**19.09**	**13.06**	**0.00**	**0.00**	**0.05**
BnaA07g24880D	*LIPOXYGENASE 2*	**1.89**	**18.74**	**23.19**	**0.21**	**0.00**	**0.04**
BnaA04g17560D	*CINNAMATE-4-HYDROXYLASE*	**27.64**	**15.61**	1.48	1.50	1.61	**90.95**
BnaC04g41120D	*CINNAMATE-4-HYDROXYLASE*	**18.56**	**3.00**	1.61	0.77	1.53	**40.45**
BnaA07g32800D	*CINNAMOYL-COA REDUCTASE*	**21.61**	**45.49**	**32.21**	1.29	**116.69**	**206.3**
BnaA08g16100D	*CYP79B2*	**1.68**	**13.03**	**9.54**	1.38	1.70	**1.99**
BnaA08g04520D	*CYP83B1*	**1.78**	**2.07**	**3.70**	0.86	0.64	0.78
BnaC04g01210D	*WRKY46*	**2.43**	**3.07**	**2.18**	1.07	**11.31**	**11.3**
BnaA04g23480D	*WRKY54*	**2.49**	**6.85**	**3.24**	1.17	**4.65**	**8.72**
BnaA09g35840D	*WRKY70*	**3.32**	**12.87**	**23.49**	1.47	**27.31**	**24.71**
BnaC06g05910D	*ANAC019*	**3.09**	**2.76**	**1.95**	**0.29**	**0.20**	**191.8**
BnaA07g28000D	*ANAC019*	**4.11**	**5.69**	**2.33**	**0.16**	1.36	**1369.3**
BnaC08g18090D	*MYB51*	**1.55**	**6.58**	**5.16**	1.03	**8.40**	**13.42**

dpi, days post-inoculation.

(*APK1*, *BnaA03g38670D*) and *APK2* (*BnaA01g34620D*, *BnaC01g00790D*, *BnaC07g51290D*). Additionally, homologs of *GLUTATHIONE SYNTHETASE 2* (*BnaA06g28850D*, *BnaC07g27830D*) were upregulated specifically in resistant hosts at 3 dpi (Data S2, Table 1). In addition to its role as a redox regulator, glutathione is a key intermediary in sulfur metabolism and the largest reservoir of non-protein reduced sulfur in the cell. It also directly serves a role in toxin neutralization through the activity of glutathione-*S*-transferases (GST). DEGs enriched for GST activity ($P = 2.77 \times 10^{-21}$) were also identified in resistant hosts at 3 dpi, including *GST PHI 2* (*GSTF2*; *BnaA03g26140D*), *GSTF6* (*BnaC05g01540D*), *GSTF12* (*BnaC09g40740D*), *EARLY RESPONSE TO DEHYDRATION 9* (*ERD9*, *BnaA06g06160D*), *ERD13* (*BnaA03g14150D*) and 26 other GSTs (Data S2).

Coordinated lignin deposition is observed in resistant cotyledons following infection with *L. maculans*

Genes coding for the formation of monolignols, *CINNAMATE-4-HYDROXYLASE* (*BnaA04g17560D, BnaC04g41120D*), *CINNAMOYL-ALCOHOL DEHEHYDROGENASE 8/ELICITOR-ACTIVATED GENE 3* (*BnaC03g61120D*) and *CINNAMOYL-COA REDUCTASE* (*BnaA07g32800D*), had a

combined average 17.6-fold increase in expression following *L. maculans* infection in resistant hosts at 3 dpi with no appreciable increase in the susceptible genotype (Table 1). Sequencing data are supported by histochemical analyses of lignin deposition at the inoculation sites of both genotypes (Figures 3e,f and S2). Resistant hosts showed prominent and coordinated deposition of lignin proximal to the site of pathogen infection and surrounding vasculature. In susceptible hosts, lignin deposition appeared uncoordinated and diffuse.

Activation of IGS biosynthetic genes and callose deposition

We identified DEGs specific to resistant cotyledons at 3 dpi that are associated with IGS biosynthetic process ($P = 5.38 \times 10^{-5}$). In resistant hosts, every gene of the IGS biosynthetic pathway was upregulated following *L. maculans* infection, whereas in the susceptible genotype several genes required for IGS production, such as *CYP79B2* and *CYP83B1* (Table 1), were downregulated during infection (Figure S3). DEGs associated with callose deposition during the defense response ($P = 1.98 \times 10^{-5}$) were also identified in resistant cotyledons at 3 dpi, and largely overlapped with the IGS biosynthetic genes and regulators described above. To visualize callose deposition, we stained infected and non-infected cotyledons with aniline blue. Callose accumulated directly adjacent to infection site of resistant cotyledons (Figure 3g), and was comparatively thin and discontinuous in susceptible hosts (Figure 3h).

The transcription factors NAC and WRKY are associated with the accelerated defense response in resistant hosts

To identify the transcription factors (TFs) associated with the accelerated defense response of resistant hosts we extracted differentially expressed TF-coding genes from the enriched GO terms: regulation of plant-type hypersensitive response ($P = 1.05 \times 10^{-95}$), intracellular signal transduction ($P = 1.54 \times 10^{-23}$) and defense response to fungus ($P = 3.03 \times 10^{-93}$) at 3 dpi. Of the 36 TF-coding transcripts (Figure S4), 19.4 and 30.5% coded for members of the NAC and WRKY TF families, respectively. We also identified IGS-promoting *MYB51*, JA-responsive JAZ TFs and *BZIP60* and *HSF-A4A* associated with the cellular heat-shock response. Although specifically activated in resistant hosts early at 3 dpi, 94.6% of these transcripts accumulated in susceptible cotyledons to levels exceeding all other treatments by 11 dpi (Figure S4). These data suggest that the timely expression of TFs may be essential for cellular reprogramming early in the defense response against *L. maculans*.

Identification of genes specifically activated by the *LepR1-AvrLepR1* gene interaction

To identify genes that specifically contribute to resistance in the *LepR1–AvrLepR1* interaction, we compared both the susceptible and resistant host transcriptomes across the infection process. We found 1221 upregulated DEGs shared at 3, 7 and 11 dpi in resistant host cotyledons (Figure 4a). We then compared the 1221 shared DEGs in resistant host cotyledons with upregulated DEGs at 3, 7 and 11 dpi in the susceptible host counterpart (Figure 4b). Of these 1221 DEGs, only 54 were exclusive to resistant host cotyledons. These 54 resistant-specific transcripts included genes involved in signal transduction and gene regulation, such as *RLP30* (*BnaA06g12220D*), *CYSTEINE-RICH RECEPTOR-LIKE PROTEIN KINASE 11* (*CRK11*, *BnaA01g12650D*), *CRK21* (*BnaAnng25570D*), *NON-INDUCIBLE IMMUNITY-INTERACTING GENE 2* (*BnaC07g23070D*) and *ETHYLENE RESPONSIVE ELEMENT BINDING FACTOR 1* (*BnaAnng 21280D*). Further, this list contains two genes associated with sulfur assimilation, *SULFATE TRANSPORTER 4.1* (*BnaA03g04410D*) and *APS-KINASE 2* (*APK2*; *BnaC07g 51290D*), and multiple IGS biosynthetic genes (Figure 4c). The complete list of 54 resistant-specific genes can be found in Table S2.

While not a host to *L. maculans*, Arabidopsis plants become susceptible to this pathogen if they are compromised in their ability to detect and/or respond appropriately (Bohman *et al.*, 2004). To functionally characterize the resistant-specific genes identified in our analyses, we challenged 49 corresponding Arabidopsis T-DNA mutants with *L. maculans* (Table S3). Seven gene disruptions resulted in a breakdown of Arabidopsis non-host resistance by 20 dpi (Figure 5b–i): *apk2-1* and *apk2-2*, deficient in production of activated sulfur required for biosynthesis of sulfur-containing secondary compounds including IGS and camalexin (Mugford *et al.*, 2009); *kunitz trypsin inhibitor 1* (*kti1*), a negative regulator of phytopathogen-induced cell death; receptors *at4g18250-1*, *at4g18250–2* and *at3g53490*; and the receptor partner *lysm-interacting kinase 1* (*lik1*). LIK1, a phosphorylation target of the chitin receptor CERK1, is associated with activation of JA-ET signaling and the repression of SA immune responses (Le *et al.*, 2014). T-DNA mutants of *PENTRATION 1* (*PEN1*), a proven regulator of non-host resistance (Nakao *et al.*, 2011), were used as a positive control and were susceptible to *L. maculans*. Wild-type Col-0 plants inoculated with *L. maculans* (Figure 5a) or water (Figure 5j) did not show any symptoms associated with infection.

Next, we measured fungal load by qPCR to confirm that lesion progression observed in the T-DNA insertion mutants was a result of *L. maculans* growth and development (Figure 5k). Fungal load was significantly greater ($P < 0.05$) in all mutants except *lik1* ($P = 0.309$) and *at3g53490* ($P = 0.462$), suggesting that the extent of lesion spread is correlated to fungal load. Other T-DNA alleles of LIK1 and At3g53490 showed no susceptibility to *L. maculans* (Table S3). This is not surprising, as the effects of T-DNA insertions on gene expression are variable (Wang, 2008) and these two mutants already display a weak

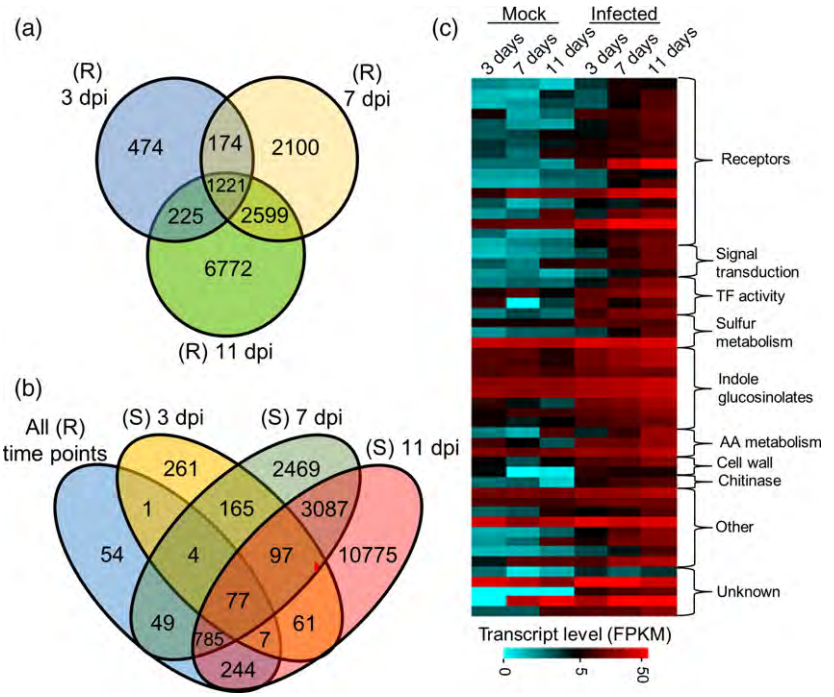

Figure 4. Identification of differentially expressed genes (DEGs) specific to resistant (R) cotyledons inoculated with *Leptosphaeria maculans*.
(a) Venn diagram showing all genes upregulated in R hosts at 3, 7 and 11 days post inoculation (dpi).
(b) Identification of DEGs specific to R hosts.
(c) Expression profiles of 54 DEGs specific to R hosts. Expression levels are measured in FPKM (fragments per kilobase of gene per million mapped reads).

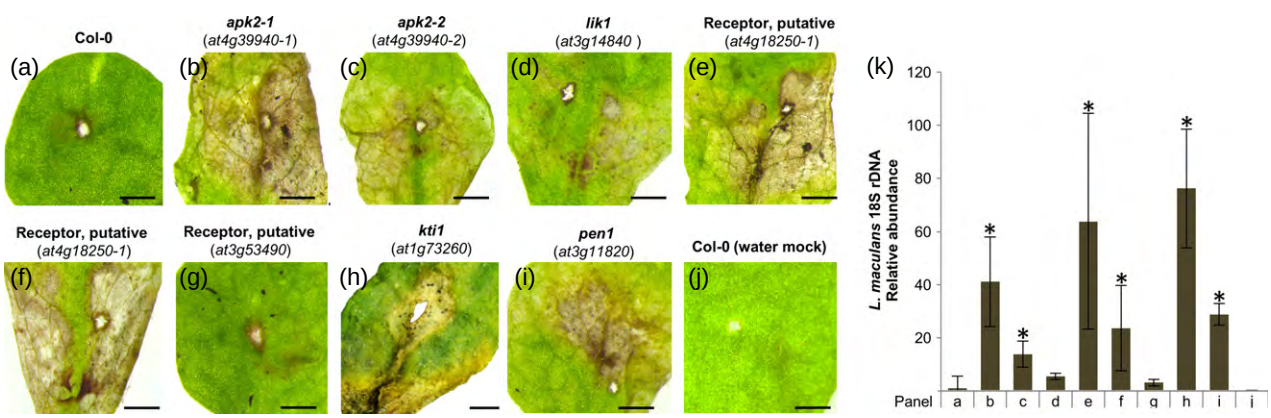

Figure 5. Disease symptoms in Arabidopsis following *Leptosphaeria maculans* infection.
(a) Wild-type Col-0, (b, c) *at4g39940.1, aps kinase 2,* (d) *at3g14840.1, lysm interacting kinase 1,* (e, f) *at4g18250.1,* putative receptor, (g) *at3g53490.1,* putative receptor, (h) *at1g73260.1, kunitz trypsin inhibitor 1,* (i) *at3g11820, penetration 1,* (j) Col-0 water inoculated mock control. Scale bar = 1 mm. (j) Relative abundance of *L. maculans* 18s rDNA in each mutant. Asterisk (*) denotes significant difference ($P < 0.05$, Student's *t*-test) in fungal load compared with Col-0.

phenotype. A complete list of screened mutants can be found in Table S3.

Laser microdissection and spatial distribution of gene activity underlying plant resistance

We then hypothesized that the resistant-specific genes identified through our transcriptome and mutant analysis would also be operative directly at the infection site to restrict spread of the pathogen into host tissues. To test this hypothesis, we used laser microdissection (LMD) coupled with quantitative PCR (qPCR) to identify how resistant-specific genes and other important defense regulators are spatially partitioned within the cotyledon directly at and distal to the infection site (Figure 6). We focused our attention on cotyledons at 7 dpi – a critical time point observed between the two genotypes in response to *L. maculans* (Figure 1b). All genes (*LIK1*, *PR1*, *WRKY25*, *PDF1.2*, *APK2*, *RBOHF*, *CYP79B2*, *BnaA03g43720D* and *BnaC04g27200D*) were highly expressed in resistant host cotyledons infected with *L. maculans* compared with the susceptible line or mock controls and further validate our sequencing data.

When resistant host cotyledons were challenged with *L. maculans*, *APK2*, *RBOHF*, *WRKY25*, *BnaA03g43720D*,

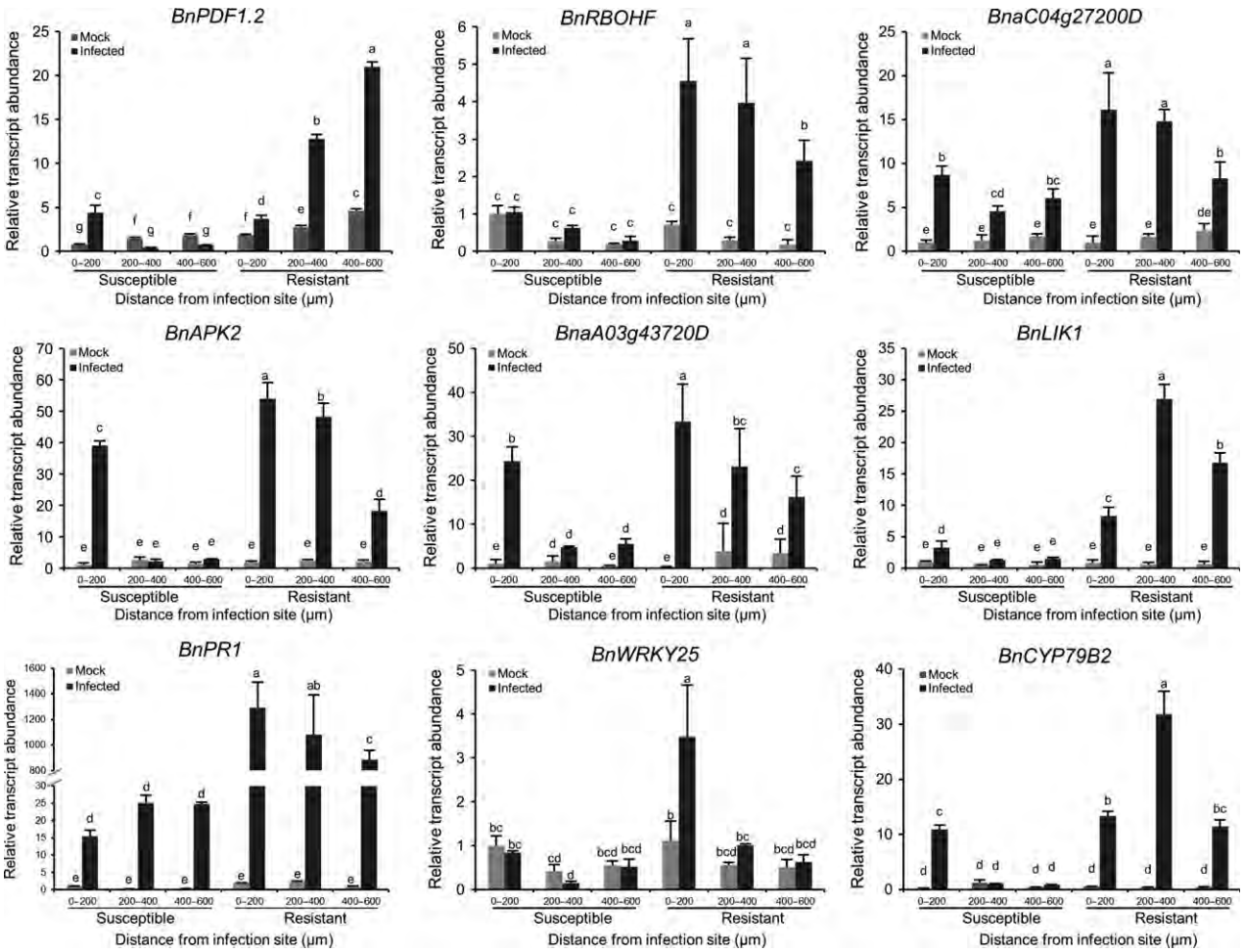

Figure 6. *Brassica napus* gene expression following inoculation with *Leptosphaeria maculans*.
Relative transcript abundance of *BnPDF1.2*, *BnRBOHF*, *BnaC04g27200D*, *BnAPK2*, *BnaA03g43720D*, *BnLIK1*, *BnPR1*, *BnWRKY25* and *BnCYP79B2* in susceptible (S) and resistant (R) cotyledons as measured 0–200, 200–400 and 400–600 μm from the inoculation site. Actin (GenBank accession number AF111812.1) was used as the internal control and to normalize expression data. Relative transcript abundance is normalized relative to S mock (0–200 μm) treatment. Error bars represent standard deviation of the mean. For each gene, different lowercase letters indicate significant differences among mean values (one-way ANOVA with Ducan's multiple range test; $P < 0.05$). The results are based on three replicates in three independent experiments.

BnaC04g27200D and the SA signaling marker *PR1* accumulated at greater levels within tissues 0–200 μm from the infection site. Levels of *LIK1* and *CYP79B2* were greatest 200–400 μm from the infection site. A marker of JA-ET signaling, *PDF1.2*, was the only transcript to accumulate highest in tissues taken distally (400–600 μm) from the infection site of resistant hosts. These data provide evidence of the spatial coordination of defense gene activity in tissues directly at the infection site in response to *L. maculans* attack.

DISCUSSION

We profiled gene expression in susceptible and resistant cotyledons of *B. napus* before, during and after infection with the hemibiotrophic fungus *L. maculans* to uncover key components of the ETD pathway. Our experiments showed an accelerated defense response in resistant host tissues coinciding with the deposition of lignin and callose that probably prevents colonization and reproduction by *L. maculans* in apoplastic spaces in canola cotyledons. Transcripts associated with resistance accumulated in gradients away from the infection site, providing unprecedented spatial resolution of the *B. napus*–*L. maculans* pathosystem.

Arabidopsis mutants of two uncharacterized receptors (*at4g18250* and *at3g53490*) were susceptible to *L. maculans*, suggesting a conserved defensive role in the Brassicaceae. Globally, accelerated defense during ETD is associated with rapid activation of RLPs, RLKs, TIR-NBS receptors and receptor partner proteins by 3 dpi involved in perception of PAMPs and observed late in the infection process in susceptible cultivars (Haddadi *et al.*, 2016). Of the receptors, 17 were specific to the resistant line and 12

were uncharacterized with no previously described host–pathogen annotation in *B. napus*, *Arabidopsis thaliana* or any other plant pathosystem (Table S2). As ETD pathways are mediated through extracellular RLPs and their associated partner proteins (Stotz *et al.*, 2014), upregulation of these receptors may produce a positive feedback loop amplifying the plant immune response and improving pathogen detection. Furthermore, if ETD and non-host resistance pathways are similar in their architecture, Arabidopsis presents a putative source of effective *R*-genes with the potential to bolster blackleg resistance in canola.

R-gene efficacy is often independent of the host cell death response (Schiffer *et al.*, 1997; Cawly *et al.*, 2005), suggesting that cell death may not always be responsible for host resistance but rather a by-product of runaway immune response or cell damage due to infection. Indeed, many necrotrophic or facultatively necrotrophic pathogens will induce host cell death mechanisms to facilitate infection (Lorang *et al.*, 2007; Kabbage *et al.*, 2013), and *L. maculans* has been shown to produce a necrosis- and ET-inducing peptide upon its biotrophic–necrotrophic transition (Haddadi *et al.*, 2016). The phytopathogen-induced cell death repressor *KTI1* was induced specifically in resistant hosts. When challenged with *L. maculans*, lesions spread rapidly in *kti* Arabidopsis plants similar to the phenotype of *accelerated cell death 2* plants described by Bohman *et al.* (2004). Although hemibiotrophic, *L. maculans* has been defined as primarily necrotrophic (Staal *et al.*, 2008) and can survive within dead or dying plant tissues. Thus, the recognition of *L. maculans* and activation of cell death regulators early in the infection process are likely to contribute to delayed onset of cell death observed during ETD. The comparative lack of these regulators early in susceptible hosts may explain its rapid lesion formation following the biotrophic–necrotrophic transition of *L. maculans.*

JA signaling has been shown to repress hypersensitive-like cell death in Arabidopsis (Rao *et al.*, 2000) and may be an overarching regulator of the genes described above. Susceptible cotyledons show a notable lag in JA response through diminished expression of integral JA biosynthetic genes *LOX2*, *AOS* and *AOC* at the time of rapid lesion spread. The expression of NAC TFs early in resistant host cotyledons may directly promote production of JA (Figure S4). For example, *NAC019* and *NAC055* promote JA-induced transcription of *LOX2* (Bu *et al.*, 2008), and *anac019anac055* double mutants are susceptible to fungal necrotrophic pathogens (Bu *et al.*, 2008).

Resistance to *L. maculans* may also involve the production of IGS. Production of IGS is required for resistance against some hemibiotrophic fungi (Hiruma *et al.*, 2013), and *in vitro* studies have shown *S*-glycosides from *B. napus*, predominantly those derived from sinigrin, are toxic to *L. maculans* (Mithen *et al.*, 1986). Our data show activation of the complete IGS biosynthetic pathway in resistant cotyledons. The production of IGS is linked to sulfur metabolism as all indole-derived phytoalexins in the brassicas contain sulfur (Pedras *et al.*, 2011). Thus, activation of genes associated with sulfur assimilation during the *LepR1–AvrLepR1* interaction supports the production of IGS. Mugford *et al.* (2009) directly linked the sulfur activator APK2 to IGS production in Arabidopsis. Although we have shown that *apk2* Arabidopsis plants are susceptible to *L. maculans*, the mechanism by which susceptibility in conferred is unclear. Other members of the IGS biosynthetic pathway that were challenged, including *cyp79b2*, *cyp79b3*, *cyp83b1* and *cypb5c*, had no discernible phenotype. The lack of a phenotype in IGS-compromised Arabidopsis plants may be due to complementation by the antifungal indole alkaloid camalexin, effective against *L. maculans* (Bohman *et al.*, 2004). As *B. napus* is unable to produce camalexin, IGS-derived phytoalexins may play an important role in defense.

We suspected that key components of the ETD pathway are likely to be spatially controlled directly at the infection site. Coordination of the ETD pathway, as revealed by LMD and qPCR, increased the spatial resolution of the dataset and demonstrated targeted activity of receptors and downstream signal transduction pathways in tissues directly in contact with and those adjacent to *L. maculans*. While hormone levels are known to flux over time during plant defense, our data show an antagonistic spatial relationship between SA and JA-ET signaling pathways established specifically in resistant host cotyledons, as indicated by the distribution of hormone markers *PR1* and *PDF1.2*.

The IGS-marker *CYP79B2* was highly expressed adjacent to the infection site in an area of combined SA and JA-ET signaling. Consistent with our dataset, Frerigmann and Gigolashvili (2014) found that expression of the main IGS-inducing TF, *MYB51*, was greatest with joint application of SA and JA. Thus, deposition of antifungal IGS-derived phytoalexins most likely does not occur in areas of direct pathogen contact but rather upstream of invading *L. maculans*, and is potentially guided by hormone gradients formed during defense.

Rapid activation of defense regulators, including TFs, in resistant hosts can contribute to the deposition of lignin, callose and other anti-fungal metabolites preceding fungal invasion. This is complemented by the ability of resistant plants to direct defense activity to the host–pathogen interface by coordinating gene expression to areas of direct fungal contact or to areas adjacent to the infection site. For example, expression of *WRKY25* in resistant host cotyledons is concentrated around 400 μm from the infection site. As a negative regulator of SA-mediated defense responses (Zheng *et al.*, 2007) and a positive regulator of ET biosynthesis (Li *et al.*, 2011), activity of WRKY25 would prevent runaway SA signaling and cell death, thus mitigating disease progression and the likelihood of colonization ny *L. maculans*.

Our data represent a valuable resource that captures gene activity following activation of ETD pathways in the *B. napus*–*L. maculans* pathosystem. The identification and characterization of genes responsible for mitigating plant disease demonstrates the utility of our dataset. Further, our data provide a preliminary framework in support of spatial transcriptional gradients responsible for plant resistance. Temporal and spatial regulation of gene expression both contribute to disease resistance, as expression of all tested genes was tightly controlled at the infection site. While many of the underlying molecular mechanisms responsible for host resistance remain unresolved, access to technologies that can dissect cells and tissues immediately at and distal to the infection site should provide clues for directed crop improvement.

EXPERIMENTAL PROCEDURES

Plant and fungal materials

Susceptible *B. napus* cultivar Westar and *B. napus* line DF78 (*Rlm3*, *LepR1*) were inoculated with *L. maculans* isolate D3 (*AvrLm5*, *AvrLepR1*; Zhang *et al.*, 2016). Canola seedlings were grown in controlled environments with a 16-h photoperiod (16°C dark, 21°C light). Plants were grown in Sunshine mix #4 (SunGro Horticulture, http://www.sungro.com/). Fungal inoculum was prepared according to Zhang *et al.* (2016). Seven-day-old seedlings were point-inoculated with 10 μl of D3 pycnidiospore suspension (2×10^7 pycnidiospores ml^{-1}) or sterilized distilled water (mock).

Microscopy, lignin and callose deposition

Cotyledons were processed for light microscopy exactly as reported in Chan and Belmonte (2013) using the Leica Historesin embedding procedure (Leica Microsystems, http://www.leica-microsystems.com/). Sections cut 3 μm thick were stained with periodic acid-Schiff's (PAS) and counterstained with toluidine blue O (TBO) for general structure. For trypan blue/aniline blue staining of fungal hyphae, fresh canola cotyledons were cleared in acetic acid: ethanol (1: 3, v/v) and stained with 0.01% trypan blue or 0.05% aniline blue in lactoglycerol (lactic acid:glycerol:distilled H_2O = 1:1:1, v/v/v). To visualize lignified plant materials, canola cotyledons were cleared in 95% ethanol and stained in phloroglucinol-HCl (a saturated solution of phloroglucinol in 20% HCl). Callose deposition was visualized using aniline blue staining. Cotyledons were incubated in K_2HPO_4 buffer for 30 min and incubated in 0.05% aniline blue using fluorescence microscopy (near UV, 395 nm). All sections and tissues were visualized on a Zeiss Axio Imager Z1 (https://www.zeiss.com/). Scanning electron micrographs were captured using the Hitachi T-1000 to examine fungal infection on the surface of freshly collected canola cotyledons without tissue fixation.

Construction of RNA sequencing libraries

RNA was collected from three biological replicates of infected and two mock inoculated *B. napus* cotyledons at 0, 3, 7 and 11 dpi. Total RNA was isolated by using PureLink® Plant RNA Reagent (Ambion, https://www.thermofisher.com) and treated with a TURBO DNA-free™ Kit (Ambion) according to the manufacturer's instructions. RNA quality and integrity was measured using the 2100 Bioanalyzer (Agilent Technologies, http://www.agilent.com/) with the Agilent 2100 PicoChip. RNA-sequencing libraries were prepared according to an alternative HTR protocol (C2) developed by Kumar *et al.* (2012), with the exception of a library PCR enrichment of 11 PCR cycles. The RNA sequencing libraries were validated using high-sensitivity DNA chips on the Agilent Bioanalyzer and quantified using the Quant-iT dsDNA Assay kit (ThermoFisher Scientific, http://www.thermofisher.com/). Fifty base pair single-end RNA-sequencing was carried out at the UC Davis genomics core facility (Davis, CA, USA) on the Illumina HiSeq 2500 platform in high-throughput mode. All data have been deposited in the Gene Expression Omnibus (GEO) data repository (accession GSE77723).

Data analysis

Barcode adaptors from the RNA sequence reads were clipped and low-quality reads removed (read quality <30) using TRIMMOMATIC software (Bolger *et al.*, 2014). Quality control of each sample was performed with FastQC reports (http://www.bioinformatics.babraham.ac.uk/projects/fastqc/). RNA sequence reads passing the quality filter were aligned to the *B. napus* genome (v.4.1; Chalhoub *et al.*, 2014) with TOPHAT2 of the Tuxedo pipeline (Trapnell *et al.*, 2012) allowing no more than two mismatches, in high-sensitivity mode, using *B. napus* reference annotation v.5.0 as a guide (Chalhoub *et al.*, 2014), and otherwise using default settings. Identification of unannotated transcripts was performed using CUFFLINKS v.2.2.1 and CUFFMERGE (Trapnell *et al.*, 2012) and transcript sequences were extracted using BEDTOOLS. Novel transcripts were identified and are defined in Data S4. Open reading frames (ORFs) were identified using TRANSDECODER (http://transdecoder.github.io) with alignment against Arabidopsis TAIR10 using NCBI BLAST (Altschul *et al.*, 1990). The BLASTp function was used when a predicted protein sequence was available, with an *E*-value cutoff of 10^{-10}. For those without a predicted ORF, or no hit, BLASTn was used to identify potential orthologs (*E*-value 10^{-10}).

CUFFQUANT, CUFFNORM and CUFFDIFF were used to generate normalized counts in FPKM (also known as RPKM in single-ended sequencing; Mortazavi *et al.*, 2008; Trapnell *et al.*, 2012) and to identify DEGs (pooled dispersion method/standard settings). Genes were considered as significantly differentially expressed with a corrected *P*-value of <0.05 (false discovery rate = 0.05). Raw counts were obtained from BAM files using the HTSeq Python Framework with the following command: 'htseq-count -m union -f bam –stranded=no input.sam bnapusannotation.gff3'. Followingn this, clustering was performed using the averaged raw counts of genes differentially expressed in one or more treatment groups. Clustering was performed with the DESeq software package (Anders and Huber, 2010). Principal component analysis was also performed with DESeq using raw counts from each individual sample and it validated clustering analysis (Figure S5).

GO term enrichment

GO term enrichment was performed according to the methods of Orlando *et al.* (2009). A hypergeometric distribution test was used to identify statistically enriched GO terms overrepresented in lists of DEG sets and assigned a *P*-value. GO terms were considered statistically enriched at $P < 0.001$. GO attributes were assigned to *B. napus* genes by transferring GO attributes of their closest putative Arabidopsis homolog (TAIR10; www.arabidopsis.org). Output from GO term enrichment can be found in Data S3.

Tissue processing for laser microdissection, RNA isolation, cDNA synthesis and qPCR

Inoculated cotyledons were collected and processed for LMD according to the methods of Belmonte *et al.* (2013). Briefly,

infection sites were cut parallel to the cotyledon petiole-like structure on either side of the lesion between 11 a.m. and 2 p.m. to minimize the time of day effect. A minimum of 16 infection sites per biological replicated were collected from the four treatments were fixed in 3:1 (v/v) ethanol:acetic acid and fixed overnight at 4°C. Tissues were then rinsed and dehydrated in a graded ethanol series (75, 85, 95, 100, 100%) followed by xylene infiltration (3:1, 1:1, 1:3 ethanol:xylene (v/v), 100% xylenes, 100% xylenes) at 4°C overnight. Tissues were washed with 100% xylene and paraffin chips were added to the xylene-infiltrated tissue and kept at 4°C overnight. Paraffin chips and tissues in xylenes were then allowed to come to room temperature (~21°C) and incubated at 42°C for 30 min followed by 60°C for 1 h. Three changes of 100% paraffin were made every hour before embedding.

Cotyledon tissues were sectioned using a Leica RM2125RT rotary microtome at 10 μm under RNase-free conditions and mounted on Leica PEN Membrane slides before being deparaffinized in xylene twice for 30 sec per wash. Histological sections 0–200, 200–400 and 400–600 μm from the edge of the infection site were collected in 60 μl of lysis buffer (Ambion, Origin). RNA was isolated from sections totaling at least 9 000 000 μm^2 (ranging from 115 to 200 microdissected sections) from at least seven individual plants exactly as reported in Belmonte *et al.* (2013). RNA quality and yield were determined using microcapillary electrophoresis (with an Agilent 2100 bioanalyzer using an RNA 6000 pico chip). Several examples of RNA traces used to assess RNA quality can be found in Figure S6. All LMD-collected tissues were of sufficient quality for downstream transcriptome profiling as described in Millar *et al.* (2015) and Chan *et al.* (2016).

Isolated RNA was converted to cDNA using the Maxima First Strand cDNA synthesis kit (ThermoFisher Scientific). Directed qPCR was carried out using a Bio-Rad CFX Connect™ Real-Time System with SYBR® Green Supermix (Bio-Rad, http://www.bio-rad.com/) as per the manufacturer's instructions in a 10-μl reaction volume. Conditions for the reaction were as follows: 95°C for 3 min, 39 cycles of 95°C for 30 sec, 53°C for 30 sec and 72°C for 30 sec. Melt curves (0.5°C increments in a 55–95°C range) for each gene were performed to assess the sample for non-specific targets, splice variants and primer dimers. A list of the primer sequences used in these experiments is given in Data S5. The ΔΔCt method was used to analyze relative transcript abundance, normalizing to the endogenous housekeeping gene *Actin* and using Westar inoculated with H_2O as a reference sample.

The ΔΔCt method was used to analyze relative mRNA abundance (Rieu and Powers, 2009). The results are based on three repeats in three independent experiments. Each biological replicate was a pool of tissue taken from at least seven individuals. Actin (GenBank accession number AF111812.1) was used as the internal control to normalize the expression of the target gene. Levels of gene expression were normalized relative to that in the Westar (0–200 μm) control.

One-way ANOVA with Ducan's multiple range test ($P < 0.05$) was performed on each gene over the three distances to test for significant fold changes between treatments ($P < 0.05$).

Arabidopsis susceptibility screening

We screened 49 loss-of-function Col-0 background Arabidopsis mutants for susceptibility to *L. maculans* (Table S3). PCR was performed to confirm homozygous insertion of the mutants. Col-0 plants were used as a resistant control line and mock water-inoculated controls were performed for all lines. Plant growth and fungal inoculation procedures were similar to that described for *B. napus* plant growth and fungal inoculation, with some modifications. Seeds were plated in MS medium in sterile conditions, then cold-treated for 3 days at 4°C, incubated in a controlled environment for 14 days and transplanted into a growth tray with growth mix. Inoculation of two similarly sized young leaves per plant was performed at the four to six leaf stage, and after inoculation a transparent plastic cover was placed over the plants to maintain high humidity. At least 30 plants from each treatment group were evaluated for blackleg resistance at 18–24 dpi and scored for disease severity.

Leaf tissue was collected in a 96-well plate from five biological replicates of Arabidopsis wild-type plants and mutants that displayed susceptibility at 20 dpi. DNA extraction buffer [1 M KCl, 100 mM 2-amino-2-(hydroxymethyl)-1,3-propanediol (TRIS)-HCl pH 7.5, 10 mM EDTA pH 8] and glass beads were added to each well and tissue was homogenized on a GenoGrinder 2000. DNA was precipitated in isopropanol, washed with 70% ethanol and suspended in TRIS-HCl pH 7.5. To properly normalize input for qPCR DNA was quantified with the Nanodrop 2000c and Quant-iT picogreen high-sensitivity dsDNA assay (ThermoFisher Scientific) on the fluorescent Nanodrop 3300. To measure 18s rDNA levels in foliar tissue, qPCR was performed with SYBR® SSO Fast Evagreen Supermix (Bio-Rad) in a 10-μl reaction volume. For each reaction, 100 pg of extracted DNA was used. Conditions for the reaction were as follows: 98°C for 3 min, 40 cycles of 98°C for 5 sec, 60°C for 10 sec. Melt curves (0.5°C increments in a 55–95°C range) for each gene were performed to assess for non-specific targets and primer dimers.

ACCESSION NUMBER

All RNA sequencing data are available from the Gene Expression Omnibus (GEO) data repository (accession GSE77723).

ACKNOWLEDGEMENTS

This work was supported through a Manitoba Agriculture Rural Development Initiatives Growing Forward 2 grant to MFB and WGDF as well as a Canola Agronomic Research Program (CARP) grant through the Canola Council of Canada to WGDF. XZ was supported by a China Council Scholarship, MGB was supported by National Science and Engineering Research Council Vanier Scholarship, and JLM by a CGS-M Scholarship.

AUTHOR CONTRIBUTIONS

XZ, MGB, MFB and WGDF conceived and designed the study. XZ and MGB wrote the manuscript. MGB, XZ, PLW, JCW, JLM, DK, MJG, JC and ACC performed experiments and interpreted and analyzed data. MFB and WGDF supervised the study and data analysis, and contributed to manuscript writing.

CONFLICTS OF INTEREST

The authors declare no conflicts of interest.

SUPPORTING INFORMATION

Additional Supporting Information may be found in the online version of this article.

Figure S1. Expression levels of hormone biosynthesis genes and hormone signaling markers in response to *Leptosphaeria maculans*.

Figure S2. Deposition of lignified plant materials at the site of infection in resistant and susceptible hosts.

Figure S3. Activation of glucosinolate and indole glucosinolate biosynthetic genes in *Brassica napus* cotyledons infected with *Leptosphaeria maculans*.

Figure S4. Transcript levels of transcription factors expressed in response to *Leptosphaeria maculans*.

Figure S5. Principal components analysis of raw counts for each individual treatment.

Figure S6. RNA quality following tissue processing and laser microdissection.

Table S1. Characterization of *R*-genes carried in line DF78 and cv. Westar.

Table S2. List of genes specifically activated in resistant line DF78 in response to *Leptosphaeria maculans.*

Table S3. Results of Arabidopsis mutant screening for susceptibility to blackleg disease.

Data S1. Gene annotation and expression levels in all treatments.

Data S2. Differentially expressed genes in cv. Westar or line DF78 following *Leptosphaeria maculans* infection.

Data S3. Gene Ontology term enrichment output.

Data S4. Genome coordinates of novel transcripts.

Data S5. Primer sequences used for laser microdissection-qPCR and 18s rDNA detection.

REFERENCES

Altschul, S.F., Gish, W., Miller, W., Myers, E.W. and Lipman, D.J. (1990) Basic local alignment search tool. *J. Mol. Biol.* **215**, 403–410.

Anders, S. and Huber, W. (2010) Differential expression analysis for sequence count data. *Genome Biol.* **11**, R106.

Belmonte, M.F., Kirkbride, R.C., Stone, S.L. *et al.* (2013) Comprehensive developmental profiles of gene activity in regions and subregions of the Arabidopsis seed. *Proc. Natl Acad. Sci. USA*, **110**, E435–E444.

Bhardwaj, A.R., Joshi, G., Kukreja, B. *et al.* (2015) Global insights into high temperature and drought stress regulated genes by RNA-Seq in economically important oilseed crop *Brassica juncea*. *BMC Plant Biol.* **15**, 9.

Bigeard, J., Colcombet, J. and Hirt, H. (2015) Signaling mechanisms in pattern-triggered immunity (PTI). *Mol. Plant*, **8**, 521–539.

Bohman, S., Staal, J., Thomma, B.P.H.J., Wang, M. and Dixelius, C. (2004) Characterisation of an *Arabidopsis-Leptosphaeria maculans* pathosystem: resistance partially requires camalexin biosynthesis and is independent of salicylic acid, ethylene and jasmonic acid signalling. *Plant J.* **37**, 9–20.

Bolger, A.M., Lohse, M. and Usadel, B. (2014) Trimmomatic: a flexible trimmer for Illumina sequence data. *Bioinformatics*, **30**, 2114–2120.

Bu, Q., Jiang, H., Li, C.-B., Zhai, Q., Zhang, J., Wu, X., Sun, J., Xie, Q. and Li, C. (2008) Role of the *Arabidopsis thaliana* NAC transcription factors *ANAC019* and *ANAC055* in regulating jasmonic acid-signaled defense responses. *Cell Res.* **18**, 756–767.

Cawly, J., Cole, A.B., Király, L., Qiu, W. and Schoelz, J.E. (2005) The plant gene CCD1 selectively blocks cell death during the hypersensitive response to Cauliflower mosaic virus infection. *Mol. Plant-Microbe Interact.* **18**, 212–219.

Chalhoub, B., Denoeud, F., Liu, S. *et al.* (2014) Early allopolyploid evolution in the post-Neolithic *Brassica napus* oilseed genome. *Science*, **345**, 950–953. Available at: http://www.sciencemag.org/cgi/doi/10.1126/science.1253435.

Chan, A. and Belmonte, M. (2013) Histological and ultrastructural changes in canola (*Brassica napus*) funicular anatomy during the seed lifecycle. *Botany*, **91**, 671–679.

Chan, A.C., Khan, D., Girard, I.J., Becker, M.G., Millar, J.L., Sytnik, D. and Belmonte, M.F. (2016) Tissue-specific laser microdissection of the *Brassica napus* funiculus improves gene discovery and spatial identification of biological processes. *J. Exp. Bot.* **67**, erw179.

Clay, N.K., Adio, A.M., Denoux, C., Jander, G. and Ausubel, F.M. (2009) Glucosinolate metabolites required for an Arabidopsis innate immune response. *Science*, **323**, 95–101.

Dangl, J.L., Horvath, D.M. and Staskawicz, B.J. (2013) Pivoting the plant immune system from dissection to deployment. *Science*, **341**, 746–751.

Denancé, N., Sánchez-Vallet, A., Goffner, D. and Molina, A. (2013) Disease resistance or growth: the role of plant hormones in balancing immune responses and fitness costs. *Front. Plant Sci.* **4**, 1–12.

Ellinger, D., Naumann, M., Falter, C., Zwikowics, C., Jamrow, T., Manisseri, C., Somerville, S.C. and Voigt, C.A. (2013) Elevated early callose deposition results in complete penetration resistance to Powdery Mildew in Arabidopsis. *Plant Physiol.* **161**, 1433–1444.

Fitt, B.D.L., Brun, H., Barbetti, M.J. and Rimmer, S.R. (2006) World-wide importance of phoma stem canker (*Leptosphaeria maculans* and *L. biglobosa*) on oilseed Rape (*Brassica napus*). *Eur. J. Plant Pathol.* **114**, 3–15.

Flor, H.H. (1971) Current status of the gene-for-gene concept. *Annu. Rev. Phytopathol.* **9**, 275–296.

Frerigmann, H. and Gigolashvili, T. (2014) *MYB34*, *MYB51*, and *MYB122* distinctly regulate indolic glucosinolate biosynthesis in *Arabidopsis thaliana*. *Mol. Plant*, **7**, 814–828.

Haddadi, P., Ma, L., Wang, H. and Borhan, M.H. (2016) Genome-wide transcriptomic analyses provide insights into the lifestyle transition and effector repertoire of *Leptosphaeria maculans* during the colonization of *Brassica napus* seedlings. *Mol. Plant Pathol.* **7**, 1196–1210.

Hiruma, K., Fukunaga, S., Bednarek, P., Pislewska-Bednarek, M., Watanabe, S., Narusaka, Y., Shirasu, K. and Takano, Y. (2013) Glutathione and tryptophan metabolism are required for Arabidopsis immunity during the hypersensitive response to hemibiotrophs. *Proc. Natl Acad. Sci. USA*, **110**, 9589–9594.

Jones, J.D.G. and Dangl, J.L. (2006) The plant immune system. *Nature*, **444**, 323–329.

Kabbage, M., Williams, B. and Dickman, M.B. (2013) Cell death control: the interplay of apoptosis and autophagy in the pathogenicity of *Sclerotinia sclerotiorum*. *PLoS Pathog.* **9**, e1003287.

Kaliff, M., Staal, J., Myrenås, M. and Dixelius, C. (2007) ABA is required for *Leptosphaeria maculans* resistance via ABI1- and ABI4-dependent signaling. *Mol. Plant-Microbe Interact.* **20**, 335–345.

Kumar, R., Ichihashi, Y., Kimura, S., Chitwood, D.H., Headland, L.R., Peng, J., Maloof, J.N. and Sinha, N.R. (2012) A high-throughput method for Illumina RNA-Seq library preparation. *Front. Plant Sci.* **3**, 1–10.

Larkan, N.J., Lydiate, D.J., Parkin, I.A.P., Nelson, M.N., Epp, D.J., Cowling, W., Rimmer, S.R. and Borhan, M.H. (2013) The *Brassica napus* blackleg resistance gene *LepR3* encodes a receptor-like protein triggered by the *Leptosphaeria maculans* effector AVRLM1. *New Phytol.* **197**, 595–605.

Larkan, N.J., Ma, L. and Borhan, M.H. (2015) The *Brassica napus* receptor-like protein RLM2 is encoded by a second allele of the *LepR3*/*Rlm2* blackleg resistance locus. *Plant Biotechnol. J.* **13**, 983–992.

Le, M.H., Cao, Y., Zhang, X.C. and Stacey, G. (2014) LIK1, a CERK1-interacting kinase, regulates plant immune responses in Arabidopsis. *PLoS ONE*, **9**, e102245.

Li, S., Fu, Q., Chen, L., Huang, W. and Yu, D. (2011) *Arabidopsis thaliana WRKY25*, *WRKY26*, and *WRKY33* coordinate induction of plant thermotolerance. *Planta*, **233**, 1237–1252.

Lorang, J.M., Sweat, T.A. and Wolpert, T.J. (2007) Plant disease susceptibility conferred by a "resistance" gene. *Proc. Natl Acad. Sci. USA*, **104**, 14861–14866.

Lowe, R.G.T., Cassin, A., Grandaubert, J., Clark, B.L., Van De Wouw, A.P., Rouxel, T. and Howlett, B.J. (2014) Genomes and transcriptomes of partners in plant–fungal-interactions between canola (*Brassica napus*) and two *Leptosphaeria* species. *PLoS ONE*, **9**, e103098.

Luna, E., Pastor, V., Robert, J., Flors, V., Mauch-Mani, B. and Ton, J. (2011) Callose deposition: a multifaceted plant defense response. *Mol. Plant-Microbe Interact.* **24**, 183–193.

Marcroft, S.J., Van de Wouw, A.P., Salisbury, P.A., Potter, T.D. and Howlett, B.J. (2012) Effect of rotation of canola (*Brassica napus*) cultivars with different complements of blackleg resistance genes on disease severity. *Plant. Pathol.* **61**, 934–944.

Meng, X. and Zhang, S. (2013) MAPK cascades in plant disease resistance signaling. *Annu. Rev. Phytopathol.* **51**, 245–266.

Millar, J.L., Becker, M.G. and Belmonte, M.F. (2015) Laser microdissection of plant tissues. In *Plant Microtechniques and Protocols* (Yeung, E.C.T., Stasolla, C., Sumner, M.J. and Huang, B.Q., eds). Cham: Springer International Publishing, pp. 337–350.

Mishra, A.K., Sharma, K. and Misra, R.S. (2012) Elicitor recognition, signal transduction and induced resistance in plants. *J. Plant Interact.* **7**, 95–120.

Mithen, R.F., Lewis, B.G. and Fenwick, G.R. (1986) *In vitro* activity of glucosinolates and their products against *Leptosphaeria maculans*. *Trans. Br. Mycol. Soc.* **87**, 433–440.

Mortazavi, A., Williams, B.A., Mccue, K., Schaeffer, L. and Wold, B. (2008) Mapping and quantifying mammalian transcriptomes by RNA-Seq. *Nat. Methods*, **5**, 1–8.

Mugford, S.G., Yoshimoto, N., Reichelt, M. *et al.* (2009) Disruption of adenosine-5′-phosphosulfate kinase in Arabidopsis reduces levels of sulfated secondary metabolites. *Plant Cell Online*, **21**, 910–927.

Nakao, M., Nakamura, R., Kita, K., Inukai, R. and Ishikawa, A. (2011) Non-host resistance to penetration and hyphal growth of *Magnaporthe oryzae* in Arabidopsis. *Sci. Rep.* **1**, 171.

Orlando, D.A., Brady, S.M., Koch, J.D., Dinneny, R. and Benfey, P.N. (2009) Manipulating large-scale arabidopsis microarray expression data: identifying dominant expression patterns and biological process enrichment. In *Plant Systems Biology* (Belostotsky, D.A., ed). Totowa, NJ: Humana Press, pp. 57–77.

Pedras, M.S.C., Yaya, E.E. and Glawischnig, E. (2011) The phytoalexins from cultivated and wild crucifers: chemistry and biology. *Nat. Prod. Rep.* **28**, 1381–1405.

Rao, M.V., Lee, H., Creelman, R.A., Mullet, J.E. and Davis, K.R. (2000) Jasmonic acid signaling modulates ozone-induced hypersensitive cell death. *Plant Cell*, **12**, 1633–1646.

Rieu, I. and Powers, S.J. (2009) Real-time quantitative RT-pcr: design, calculations, and statistics. *Plant Cell Online*, **21**, 1031–1033.

Rouxel, T., Penaud, A., Pinochet, X., Brun, H., Gout, L., Delourme, R., Schmit, J. and Balesdent, M.H. (2003) A 10-year survey of populations of *Leptosphaeria maculans* in France indicates a rapid adaptation towards the *Rlm1* resistance gene of oilseed rape. *Eur. J. Plant Pathol.* **109**, 871–881.

Šašek, V., Nováková, M., Jind, B., Bóka, K., Valentová, O. and Burketová, L. (2012) Recognition of avirulence gene *AvrLm1* from hemibiotrophic ascomycete *Leptosphaeria maculans* triggers salicylic acid and ethylene signaling in *Brassica napus*. *Mol. Plant-Microbe Interact.* **25**, 1238–1250.

Schiffer, R., Görg, R., Jarosch, B., Beckhove, U., Bahrenberg, G., Kogel, K. and Schulze-Lefert, P. (1997) Tissue dependence and differential cordycepin sensitivity of race-specific resistance responses in the barley-powdery mildew interaction. *Mol. Plant-Microbe Interact.* **10**, 830–839.

Staal, J., Kaliff, M., Bohman, S. and Dixelius, C. (2006) Transgressive segregation reveals two Arabidopsis TIR-NB-LRR resistance genes effective against *Leptosphaeria maculans*, causal agent of blackleg disease. *Plant J.* **46**, 218–230.

Staal, J., Kaliff, M., Dewaele, E., Persson, M. and Dixelius, C. (2008) RLM3, a TIR domain encoding gene involved in broad-range immunity of Arabidopsis to necrotrophic fungal pathogens. *Plant J.* **55**, 188–200.

Stotz, H.U., Mitrousia, G.K., de Wit, P.J.G.M. and Fitt, B.D.L. (2014) Effector-triggered defence against apoplastic fungal pathogens. *Trends Plant Sci.* **19**, 491–500.

Thomma, B.P.H.J., Numberger, N. and Joosten, M.H.A.J. (2011) Of PAMPs and effectors: the blurred PTI-ETI dichotomy. *Plant Cell*, **23**, 4–15.

Trapnell, C., Roberts, A., Goff, L. *et al.* (2012) Differential gene and transcript expression analysis of RNA-seq experiments with TopHat and Cufflinks. *Nat. Protoc.* **7**, 562–578.

Tsuda, K. and Katagiri, F. (2010) Comparing signaling mechanisms engaged in pattern-triggered and effector-triggered immunity. *Curr. Opin. Plant Biol.* **13**, 459–465.

Van de Wouw, A.P., Cozijnsen, A.J., Hane, J.K., Brunner, P.C., McDonald, B.A., Oliver, R.P. and Howlett, B.J. (2010) Evolution of linked avirulence effectors in *Leptosphaeria maculans* is affected by genomic environment and exposure to resistance genes in host plants. *PLoS Pathog.* **6**, e1001180.

Wang, Y.H. (2008) How effective is T-DNA insertional mutagenesis in Arabidopsis? *J. Biochem. Technol.* **1**, 11–20.

Zhang, X., Peng, G., Kutcher, H.R., Balesdent, M.H., Delourme, R. and Fernando, W.G.D. (2016) Breakdown of *Rlm3* resistance in the *Brassica napus*–*Leptosphaeria maculans* pathosystem in western Canada. *Eur. J. Plant Pathol.* **145**(3), 659–674.

Zheng, Z., Mosher, S.L., Fan, B., Klessig, D.F. and Chen, Z. (2007) Functional analysis of Arabidopsis WRKY25 transcription factor in plant defense against *Pseudomonas syringae*. *BMC Plant Biol.* **7**, 2.